SHARE

SEVENTH FRAMEWORK PROGRAMME

Grant Agreement no. 226967
Seismic Hazard Harmonization in Europe
Project Acronym: SHARE

SP 1-Cooperation

Collaborative project: Small or medium-scale focused research project

THEME 6: Environment

Call: ENV.2008.1.3.1.1 Development of a common methodology and tools to evaluate earthquake hazard in Europe

Deliverable 2.7 – Preliminary Reference Euro-Mediterranean Seismic Hazard Zonation

Due date of deliverable: 30.11.2012
Actual submission date: 18.07.2013

Start date of project: 2009-06-01 Duration: 36

Swiss Seismological Service, Eidgenössische Technische Hochschule (SED-ETHZ)

NAMES INVOLVED : G. Weatherill, H. Crowley, Danciu, L.

Revision: 2

Dissemination Level		
PU	Public	x
PP	Restricted to other programme participants (including the Commission Services)	
RE	Restricted to a group specified by the consortium (including the Commission Services)	
CO	Confidential, only for members of the consortium (including the Commission Services)	

1. Introduction

1.1 Seismic Zonation

The representation of seismic hazard input in earthquake resistant design codes is a critical interface between the scientific and engineering communities in the process of effective earthquake mitigation. When adopting a probabilistic approach of seismic hazard analysis it is necessary to identify the pertinent information emerging from the calculations that is of practical significance for engineering design. In practice, however, the process has often been limited by the means of dissemination implementation. It is within this context that the concept of "seismic zonation" emerges.

Seismic zonation, as it relates to engineering design, separates a region into areas of similar seismic hazard for which uniformity in the level and character of seismic input can be assumed for the purposes of design. In reality, this may represent a simplification of the full hazard model, as it is rendering information that exists in a continuum onto a set of discrete and uniform zones. To minimise the disparity in seismic design performance within a zone, it is suggested here that a zonation should take into account multiple characteristics of the hazard, and not necessarily only the level of ground acceleration at a single return period. Seismic zonations of this sort are becoming more widely adopted in building design codes across the globe (see Weatherill *et al*., (2010) and references therein). The evolution of design codes to meet multiple performance objectives is a driving factor in defining zonations that are created to describe, more comprehensively, the spatial variation in seismic hazard.

This report presents an analysis of the present characterisation of the seismic hazard input in the Eurocode 8, and demonstrates the variation of controlling parameters on a spatial scale when compared with the current results of the SHARE model. In addition, potential methods to assist in constraining controlling parameters of the design spectrum are explored.

1.2 Objectives of the Preliminary Reference Zonation

In section 4 of this report a preliminary reference zonation is presented. This demonstrates the concept of a "multi-objective" zonation, one in which multiple sources of hazard information are used to guide the delineation of the seismic zones. For the purposes of practical comparison against existing requirements, the return period of reference remains as 475 years.

1.3 Disclaimer

The results of this analysis and the preliminary reference zonation shown in this report represent the outcomes of a critical investigation into the nature of seismic hazard characterisation in Europe, in the context of Eurocode 8 specifications. The considerable volume of information and range of outputs from the SHARE analysis provide an excellent basis for investigating how design code requirements compare with seismic hazard on a pan-European scale. The results shown herein have been presented to, and discussed with, members of the Eurocode 8 drafting committee. It must be recognised, however, that where conclusions are drawn regarding the suitability of current recommended parameters, these represent the opinions of the authors of this report, and should not in themselves form a basis for policy without external scrutiny from members of the national authorities responsible for drafting standards in the participating Eurocode countries. Provisional recommendations for updates and changes to seismic design inputs in Eurocode 8 can be found in SHARE Deliverable 2.6 (Crowley *et al*., 2013).

2. Hazard Zonation for Seismic Design – Current Status in the Euro-Mediterranean Region

2.1. Current Status of Zonations

The current status of seismic hazard zonations for the purposes of existing design codes in Europe has been reviewed comprehensively in the report of Solomos *et al.* (2008), and many of the corresponding hazard studies discussed in Garcia-Mayordomo *et al.* (2004). For the purposes of completeness the reader is referred to the compilation found in Solomos *et al.* (2008).

2.2. Summary of Seismic Hazard Data from the SHARE Analysis

In accordance with the requirements specified in Deliverable 2.1, the SHARE project has produced the following seismic hazard outputs:

1. Seismic Hazard Curves for each site for the following intensity measures: PGA, Sa (0.1 s), Sa (0.2 s), Sa (0.3 s), Sa (0.5 s), Sa (1.0 s), Sa (2.0 s), Sa (3.0 s), Sa (4.0 s)
2. Uniform Hazard Spectra for each site for the following return periods: 95 years, 225 years, 475 years, 2475 years
3. Seismic Hazard Maps for each intensity measure listed in (1) and for each return period listed in (2)
4. Disaggregation for selected sites, including Basel, Bergen, Bucharest, Istanbul, Koln, L'Aquila, Lisbon, Rhodos, Thessaloniki, Wien

Due to the considerable computational cost required in calculating the disaggregation, it has only been possible within the timeframe of the project to produce the disaggregation for selected sites, and not across the entire region, as was initially envisaged in Deliverable 2.1. Whilst the potential usages of the disaggregation will be considered, and illustrated where appropriate, it has not been possible to define a European-wide methodology for zonation that takes into consideration the controlling earthquakes of the hazard. However, the full hazard curves and uniform hazard spectra for each site allows for the consideration of spectral parameters and performance-based seismic design requirements within the seismic zonation process. This may help extend the approaches to zonation beyond simple consideration of PGA at a fixed return period.

Also requested in Deliverable 2.1 were seismic hazard maps of PGV and PGD (or an appropriate proxy). In the case of PGD it was recognised that the requirement of a very long period spectral displacement limited the selection of the GMPEs in a manner that was inconsistent with the approach taken by Work Packages 4 and 5 of this project in creating the GMPE logic tree. Therefore it is not possible at present to determine maps of PGD. PGV presented a similar problem, particularly in stable continental regions where few existing GMPEs describe coefficients for the estimation of PGV. The decision was therefore taken to use the 0.5 s spectral acceleration as a proxy for PGV where it has not been defined in the GMPE, as suggested by Bommer & Alarçon (2006). For the design applications of PGV the invocation of a proxy may be sufficient. In order to test the use of PGV/PGA in defining the zonation, in the manner outlined by Bommer *et al.* (2010), the use of a proxy PGV may result

in an unfair framework for testing the method. Instead it may be preferable to limit the testing of the PGV/PGA ratio method to a particular branch of the logic tree, or to a region type where no PGV proxies were invoked.

The analyses presented in here utilise only the hazard maps, curves and uniform spectra from the mean of the SHARE logic tree. At the time of writing neither the higher fractiles of the logic tree, not the results of the disaggregation analysis are yet available. These outputs will be released in the months subsequent to this publication and may be integrated into the analysis in due course. However, neither of these additional outputs would be expected to alter the results presented here. In addition, the final SHARE logic tree considers three different branches for the source model: i) a uniform area source branch (AS), ii) a branch considering fault geology plus background seismicity (FBS), iii) a model derived from smoothed seismicity (SS). The decision has been taken to adjust the weightings of the branches depending on the return period of the hazard map under consideration, with shorter return periods weighted with AS:FBS:SS as 0.45:0.1:0.45, intermediate return periods (including the 475 year return period) as 0.5:0.2:0.3, and longer return periods 0.6:0.3:0.1. In the current analysis, the results are influenced not only by the variation in hazard across the spectral period range, but also by the return period range. To adopt the approach described here would lead to inconsistencies in the scaling of the hazard, particularly relevant for section 4, so therefore only the intermediate scenario (0.5:0.2:0.3) is considered.

3. Defining the Eurocode 8 Parameters across Europe

3.1. The Eurocode 8 Design Spectrum and Summary of Requirements

To place the following results in context, the Eurocode 8 seismic design provisions are summarised as follows:

3.1.1. Return Period and Performance Requirements

Eurocode 8 defines the seismic action input in terms of the Peak Ground Acceleration on reference (Type A) bedrock (a_{gR}). For the performance requirements the following return periods are defined as recommended parameters in EN1998-1 ("General Rules, Seismic Actions and Rules for Buildings") and EN1998-3 ("Assessment and Retrofitting of Structures"):

*Table 3.1: Performance-Based Seismic Design objectives and limit states defined in **EN 1998-1***

Requirement	Return Period
"Limit State of Near Collapse" (**EN 1998-3 2.1.3(P)**)	2475 years (2 % POE in 50 years)
"No-Collapse" (**EN1998-1 2.1.1(P)**) / "Limit State of Significant Damage" (**EN 1998-3 2.1.3 (P)**)	475 years (10 % POE in 50 years)
"Limit State of Damage Limitation (**EN 1998-3 2.1.3(P)**)	225 years (20 % POE in 50 years)
"Damage Limitation" (**EN1998 2.1.1(P)**)	95 years (10 % POE in 10 years)

3.1.2. Horizontal Elastic Response Spectrum

The elastic response spectrum, illustrated in Figure 3.1, is clearly defined for the horizontal components of seismic action from the following equations (**EN 1998-1 3.2.2.2 (1)P**):

$$0 \le T \le T_B:\ S_e(T) = a_g \cdot S \cdot \left[1 + \frac{T}{T_B} \cdot (\eta \cdot F_0 - 1)\right] \quad (3.1a)$$

$$T_B \le T \le T_C:\ S_e(T) = a_g \cdot S \cdot \eta \cdot F_0 \quad (3.1b)$$

$$T_C \le T \le T_D:\ S_e(T) = a_g \cdot S \cdot \eta \cdot F_0 \cdot \left[\frac{T_C}{T}\right] \quad (3.1c)$$

$$T_D \le T \le 4.0s:\ S_e(T) = a_g \cdot S \cdot \eta \cdot F_0 \cdot \left[\frac{T_C T_D}{T^2}\right] \quad (3.1d)$$

where:

- $S_e(T)$ is the elastic response spectrum (i.e., pseudo-spectral acceleration at vibration period T of a linear single-degree-of-freedom system)

- a_g is the design peak ground acceleration defined as the product of reference ground acceleration $a_{g,R}$ and importance factor γ_I.
- S is the soil factor
- η is the damping correction factor with a reference value of $\eta = 1$ for 5 % viscous damping
- F_0 is an effective amplification factor, which is fixed at 2.5 for all soil conditions.

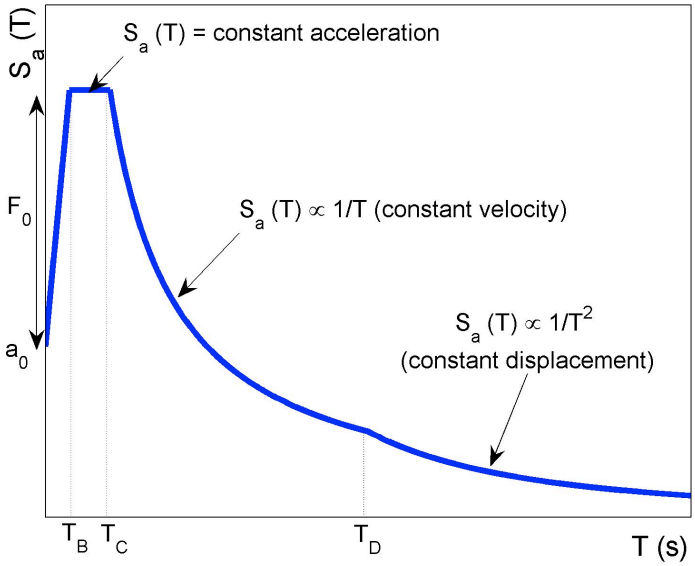

Figure 3.1: Construction of the Eurocode 8 design spectrum

The shape of the curve is fixed by four points (a_g, T_B, T_C and T_D), and response acceleration is presented as the ratio of the pseudo-spectral acceleration to the site-adjusted peak ground acceleration, $a_{gR}.S$ (hence $S_e(0) = 1$). The lower limit of the constant acceleration part of the spectrum is given by T_B, and the upper limit by T_C. The third parameter is T_D, which marks the lower limit of the constant spectral displacement part of the spectrum.

The recommendations provided in **EN 1998-1** define two types of elastic response spectrum (Type 1 and Type 2). The former is intended to be applied when the surface-wave magnitude of the controlling earthquake is greater than or equal to M_S 5.5, the latter when it is less than M_S 5.5. The spectrum corner parameters (S, T_B, T_C and T_D) are defined for each soil type in the manner shown in Table 3.1

*Table 3.1: Site and corner periods for the **EN 1998-1** ERS*

	Type 1 Spectrum ($M_S \geq 5.5$)				Type 2 Spectrum ($M_S < 5.5$)			
Ground Type	S	T_B (s)	T_C (s)	T_D (s)	S	T_B (s)	T_C (s)	T_D (s)
A	1.0	0.15	0.4	2.0	1.0	0.05	0.25	1.2
B	1.2	0.15	0.5	2.0	1.35	0.05	0.25	1.2
C	1.15	0.2	0.6	2.0	1.5	0.1	0.25	1.2
D	1.35	0.2	0.8	2.0	1.8	0.1	0.30	1.2
E	1.4	0.15	0.5	2.0	1.6	0.05	0.25	1.2

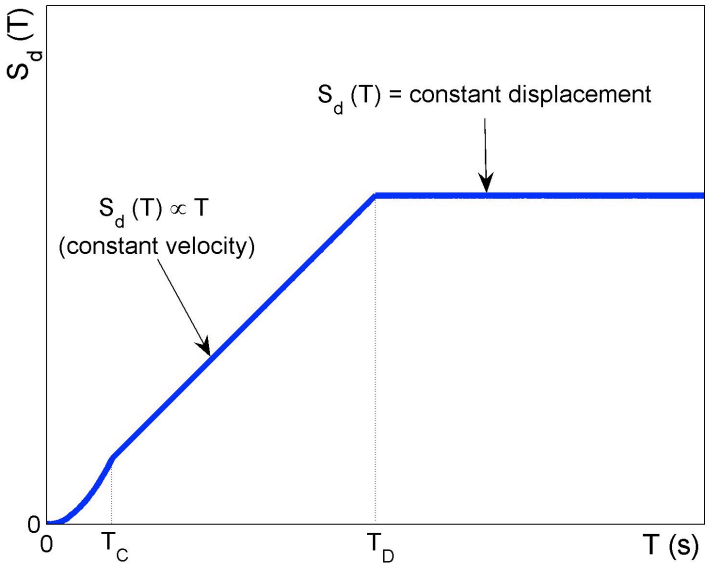

Figure 3.2: Construction of the Eurocode 9 design displacement spectrum

In addition to the definition of the design spectrum for acceleration, Eurocode 8 provides the means by which the spectral displacement ($S_{De}(T)$) is determined:

$$S_{De}(T) = S_e(T)\left[\frac{T}{2\pi}\right]^2 \tag{3.2}$$

The corresponding design spectrum is shown in Figure 3.2, which illustrates more clearly the role of the corner period T_D in defining the onset of the constant spectral displacement part of the design spectrum. It is also evident that as the influence of T_D on the acceleration design spectrum is limited, it may be necessary to seek methods of estimating T_D that are independent of the remaining corner periods of the design spectrum

3.2. Seismic Hazard Maps for the Euro-Mediterranean Region on Bedrock

Figures 3.3 – 3.5 show the seismic hazard maps from the SHARE Area Source model for the 475-year, 95 year and 2475 year return periods, for peak ground acceleration. Additional maps showing spectral accelerations and other intensity measures are presented in the following discussion where relevant.

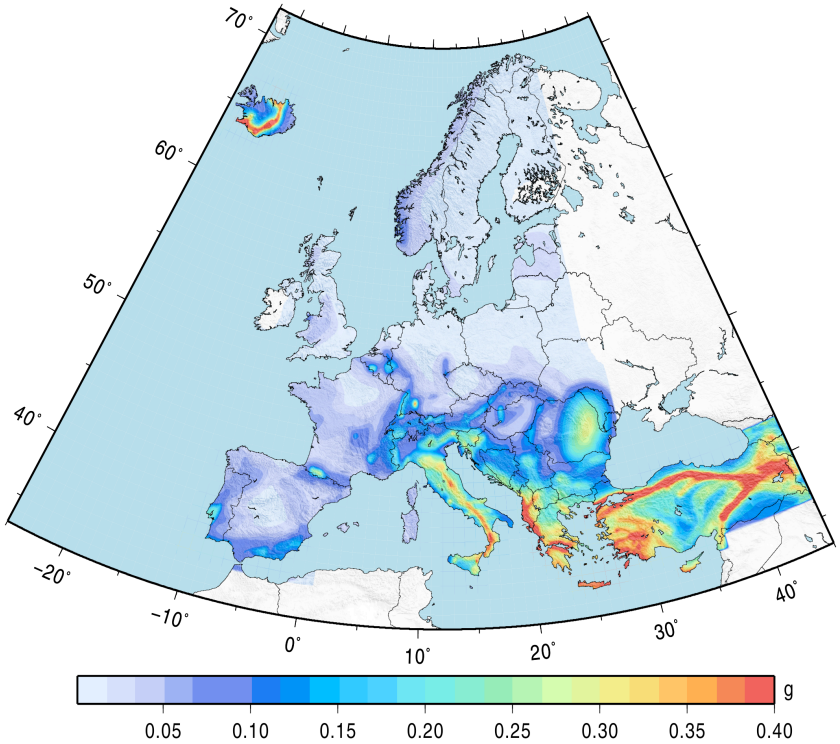

Figure 3.3a Peak Ground Acceleration on Reference (Type A) Bedrock (a_{gR}) with a 10 % probability of being exceeded in 50 years (475 year return period)

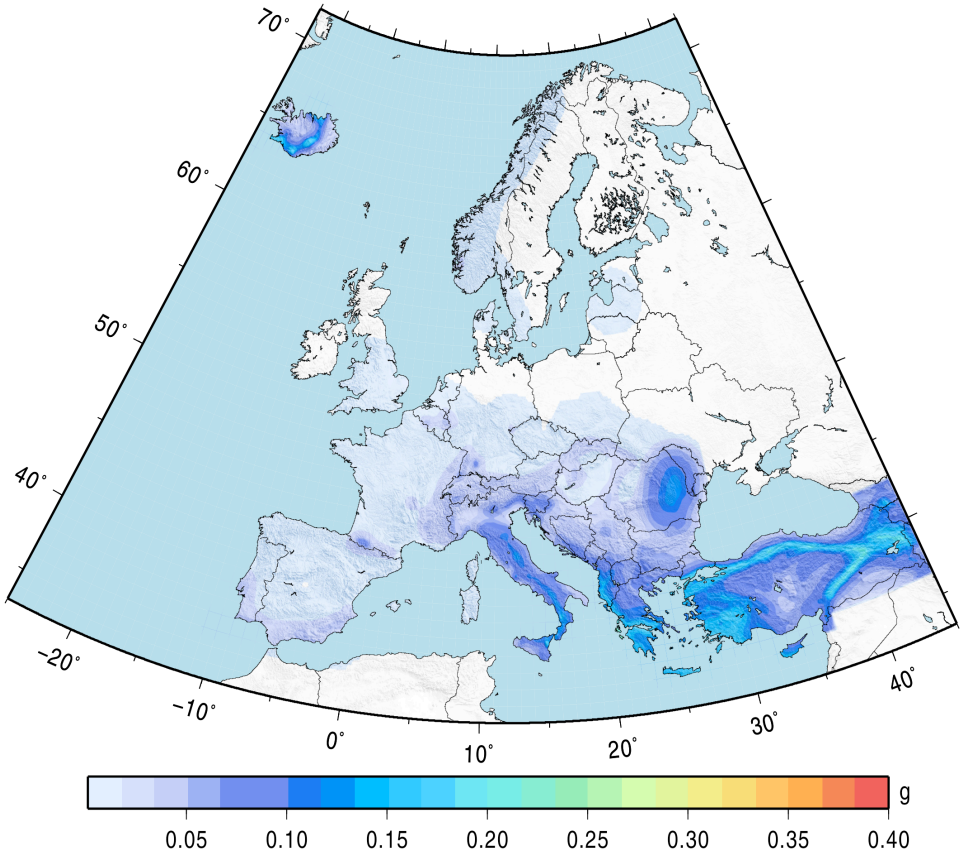

Figure 3.3b: Peak Ground Acceleration on Reference (Type A) Bedrock (a_{gR}) with a 10 % probability of being exceeded in 10 years (95 year return period)

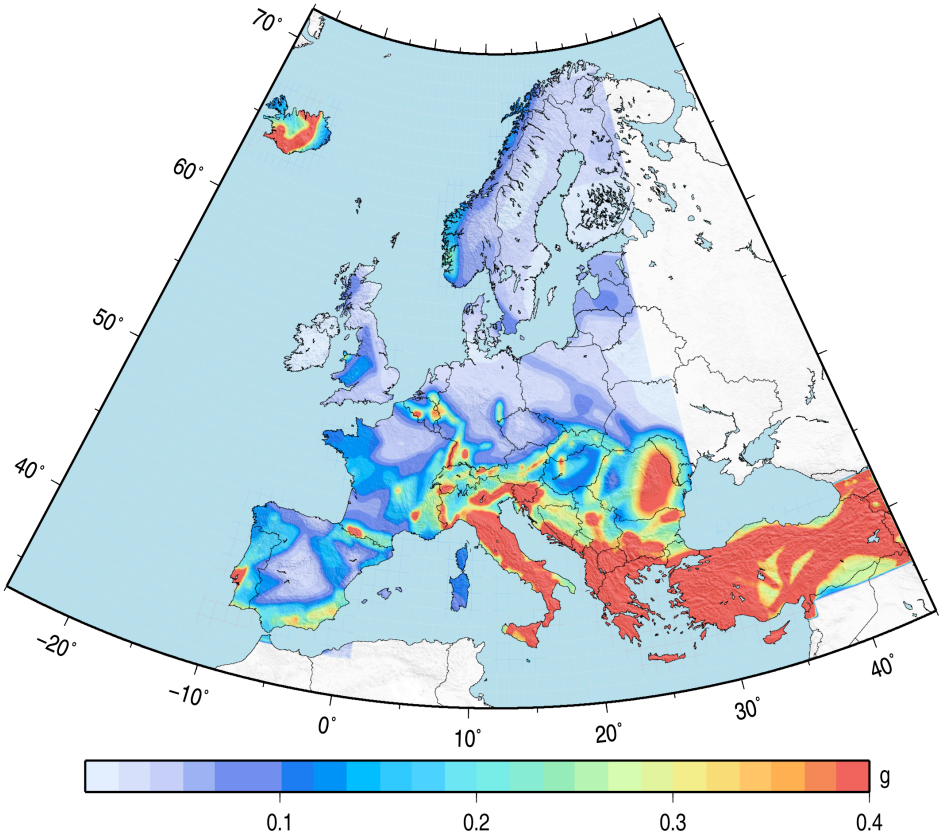

Figure 3.3c: Peak Ground Acceleration on Reference (Type A) Bedrock (a_{gR}) with a 2 % probability of being exceeded in 50 years (2475 year return period)

3.3. Calculating the Spectrum Controlling Parameters F_0, T_B and T_C

3.3.1 Methodology

As indicated in section 3.1, the shape of the design spectrum, whilst anchored to the a_g, is controlled by three corner periods T_B, T_C and T_D and an amplification factor F_0. The corner period demarcating the constant displacement part of the elastic spectrum (T_D) represents a special case, which will be addressed in the next section. In the context of seismic design, the Eurocode 8 design spectrum is intended as a basis for practical performance-based methodologies, it is therefore interpreted in such a manner that exceedance of the acceleration level for any given period is equally probable. This is, in effect, representative of a uniform hazard spectrum (UHS).

The intention behind the following methodology is to constrain the parameters of the design spectrum for each site, such that the difference between the uniform hazard spectrum and the code based design spectrum at any given site is minimised. The output of the SHARE seismic hazard analysis provides uniform hazard spectra for a total of 126,044 sites across Europe, of which 83,350 are located onshore (excluding the Azores (Portugal), Greenland and any non-European overseas territories). To determine the corner periods for such a large number of sites a constrained optimisation algorithm is applied to each site. For this purpose the Sequential Least-Squares Quadratic Programming (SLSQP) algorithm is implemented from

the SciPy (Scientific Python) numerical analysis package. As a derivative-free constrained optimisation method, the algorithm allows us to minimise the objective function (*f(x)*) subject to both parameter bounds and inequality constraints. In this particular case *f(x)* represents the weighted sum-of-squares difference between the observed UHS and the design spectrum:

$$f\left(x\right) = \sum_{i=1}^{N_{periods}} w_i \left(Sa\left(T_i\right)^{DES} - Sa\left(T_i\right)^{UHS} \right)^2 \tag{3.3}$$

Where $Sa(T_i)^{UHS}$ is the uniform hazard at period T_i, and $Sa(T_i)^{DES}$ is the expected design spectrum as period T_i, evaluated using (3.1). The design spectrum is anchored to a_{gR}, and both S and η are fixed at unity (i.e. we are considering the spectral acceleration at 5 % damping on reference bedrock). Several weighting schemes were considered and the performance of the algorithm was not significantly different from a uniform weighting ($w_i = 1$). The four free parameters are therefore F_0, T_B, T_C and T_D. The optimisation is subject to the following parameter bound constraints:

i. $\{F_0, T_B, T_C, T_D\} > 0$
ii. $(T_C - T_B) > 0$
iii. $(T_D - T_C) > 0$ (by induction $(T_D - T_B) > 0$)

To illustrate the comparative fit of the algorithm to the input UHS, examples from selected low and high seismicity sites are shown in Figure 3.4. In these examples the UHS have been constructed using linear interpolation between the ten spectral periods used in the calculation. As a consequence the observed UHS is clearly coarse. To overcome this, the UHS were interpolated onto a finer resolution (0.01 s) using a cubic radial basis function applied in log-log space. It is the interpolated UHS to which the data is fit. Obviously, the definition of the UHS itself would be improved by the inclusion of more spectral periods, but this will of course incur an additional computational cost. In general, the fit of the design spectra to the UHS shown in Figure 3.4 would suggest reliability in this approach, although some anomalies can occur in very low hazard regions.

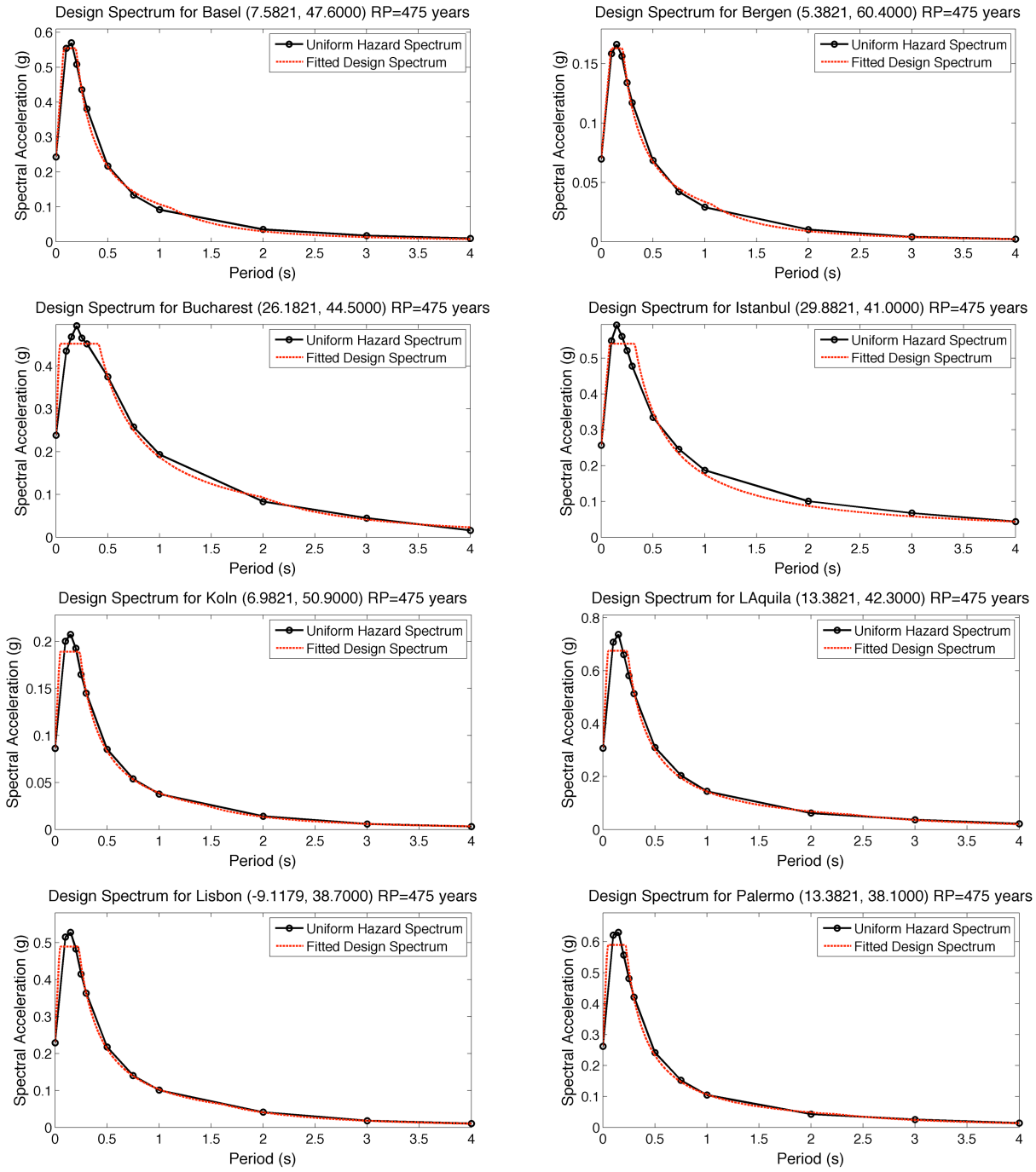

Figure 3.4 Example comparisons of the UHS and the Eurocode 8 style of the design spectrum fit by optimisation of F_0, T_B, T_C and T_D (continued ...)

The spatial distribution of the parameters F_0, T_B, T_C and, for completeness, T_D, is shown in Figures 3.5 to 3.8. For some low seismicity sites, it was not possible to fit parameters to the UHS owing to saturation of the hazard curves at high probabilities.

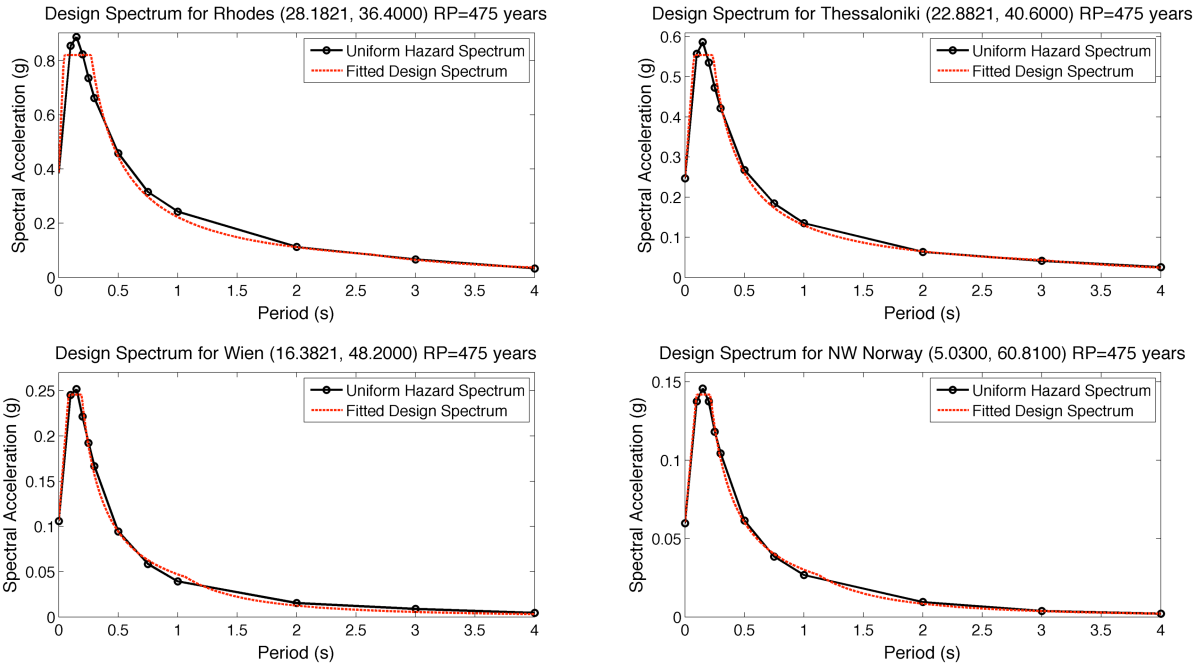

Figure 3.4 ... continued

The result maps of the four parameters present some challenges in interpretation, and some care is needed in doing so. For F_0 the clearest distinction in the maps is that between northwestern Europe (low seismicity) and the Mediterranean (high seismicity), in which higher F_0 values are found in the regions of higher seismicity. This trend is evident in the UHS shown in Figure 3.4, for which the low seismicity sites of Koln and Bergen show surprisingly less amplification at the 0.2 s period than for the higher seismicity sites. This pattern runs contrary to what is expected, as in low seismicity regions one might expect higher amplification due to the greater influence of smaller near-field events on the site, which typically display relatively higher short period accelerations.

The maps of T_B and T_C are particularly difficult to interpret, as the trends are not clearly aligned with major features of the seismicity and tectonics of the region. It is also evident from the UHS comparisons in Figure 3.4, that the relative coarseness of the UHS will have a significant influence here. For much of Europe, particularly in the moderate-high seismicity regions the value of T_B seems to stabilise around 0.06 – 0.08 s. Several low seismicity areas seem to indicate a much higher value of T_B, on the order of 0.16 – 0.2 s. It is certainly possible that this anomaly is due to poor fitting of the design spectrum to the UHS, although when considering the UHS shown in Figure 3.4 it is not obvious from inspection that this is the case. In general this trend can simply be ascribed to the shape of the UHS, which is producing a narrower peak at 0.2 s. In order to fit this with an idealised design spectrum, it procedure has raised T_B and accordingly lowered T_C.

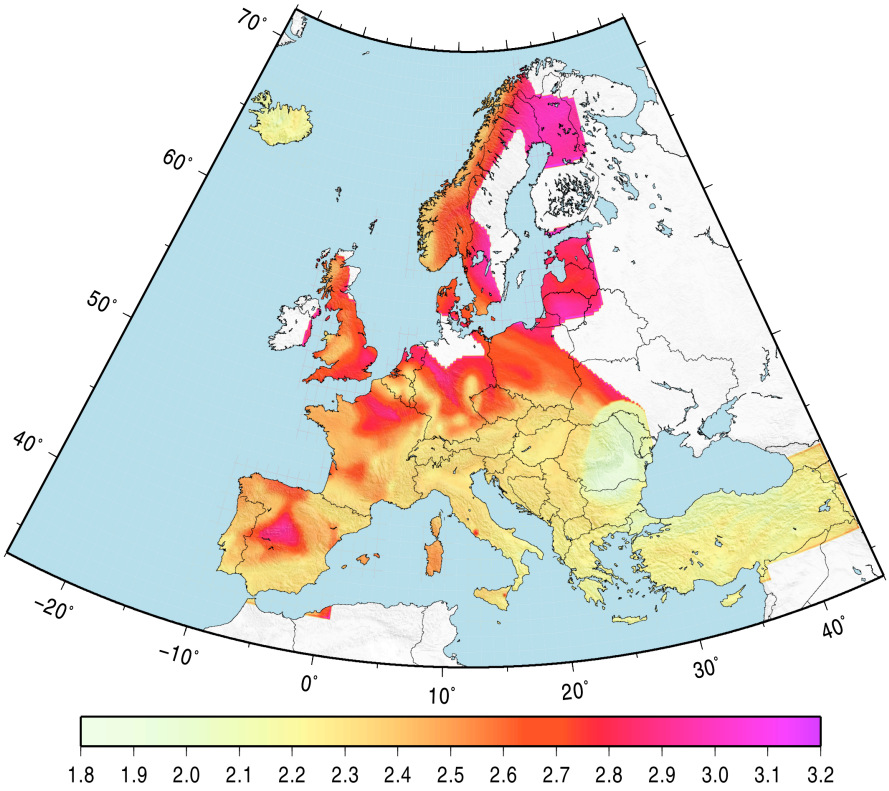

Figure 3.5: Spectral amplification factor F_0 derived from the SHARE model for the 475-year return period

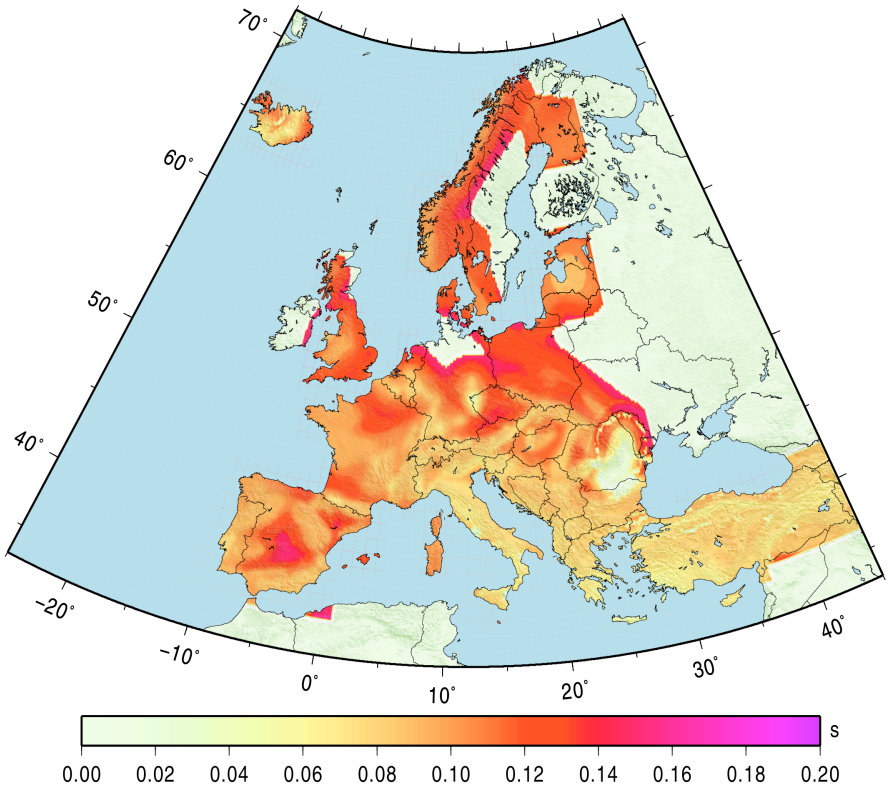

Figure 3.6: Constant acceleration corner period T_B derived from the SHARE model for the 475-year return period

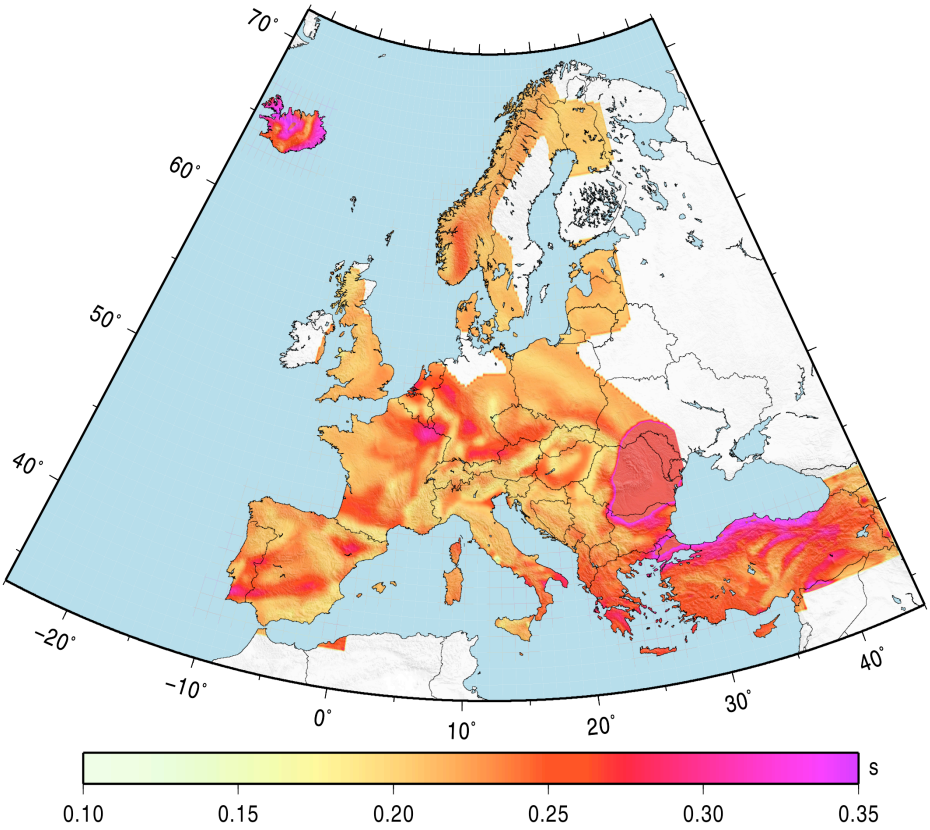

Figure 3.7: Constant velocity corner period T_C derived from the SHARE model for the 475-year return period

For the maps of T_C there are perhaps some more consistencies with the tectonics of the various regions. Obviously the highest values of T_C are found in Romania where hazard is coming principally from deep large events, much richer in low frequency motion due to the size of the rupture and the attenuation characteristics of such deep events. In mainland Europe the highest T_C values seem to be originating from areas that are moderate distances (40 – 60 kilometres or more) from large active sources. This can be seen in places such as eastern Portugal, the low-countries (away from the Rhine Graben), northern Greece and the north coast of Turkey. Interestingly, other places of moderate to high seismic activity, such as central Italy and Southern Spain, have low values of T_C. This appears to be due to a narrow constant-acceleration segment of the design spectrum, which is itself attributable to the narrow peak of the UHS, as is illustrated for L'Aquila in Figure 3.4.

The results for F_0, T_B and T_C provide some important context in looking at how the shape of a design spectrum may vary across Europe. It must be recognised, however, that the method shown here may be subject to its own biases and inconsistencies. The limitations that arise from the relatively poorly sampled uniform hazard spectrum may obscure features that are relevant for the definition of the code design spectrum. Furthermore, like any constrained optimisation methodology, there will often be cases where the optimisation has stabilised prematurely at a sub-optimum result. Certainly it is recommended that when considering the spatial variation on a more local to national scale it would be preferable to reapply the methodology and investigate the possible influences of the parameter selection or different strategies for optimisation. Likewise, further site-by-site comparisons with the modelled UHS

and the disaggregation values should also be implemented as a crucial check on the predicted corner periods.

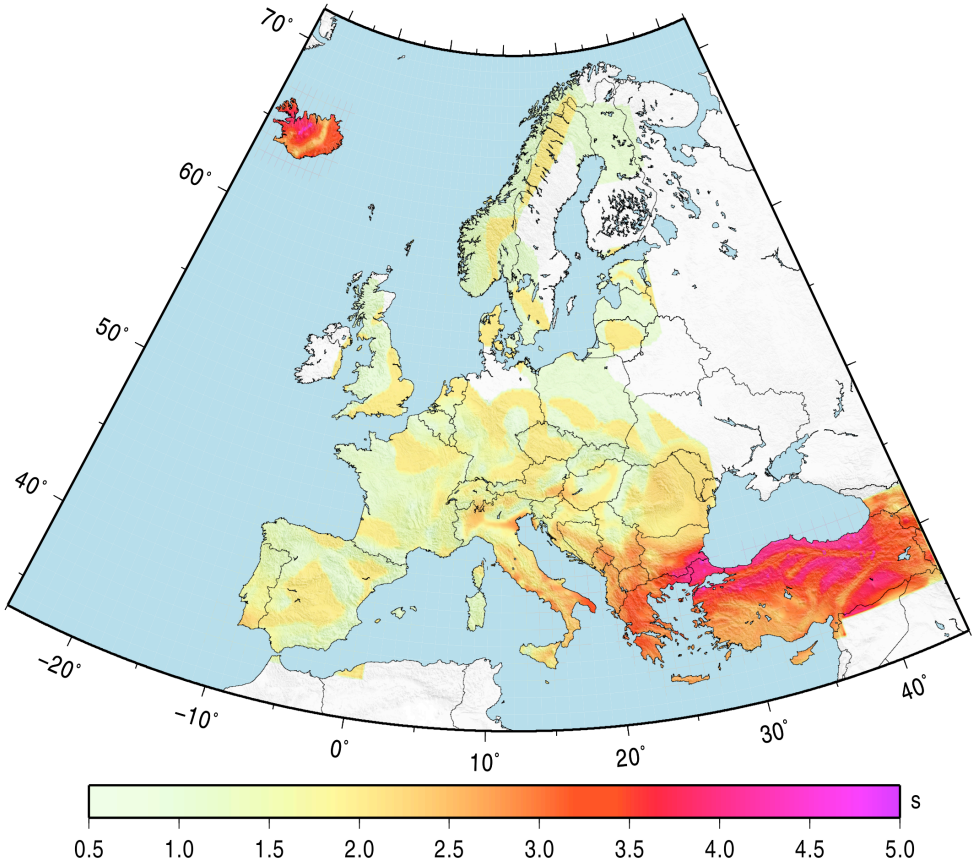

Figure 3.8: Constant displacement corner period T_D derived from the SHARE model for the 475-year return period

3.3. T_D

The constant displacement corner period T_D was included within the optimisation to provide consistency with the definitions given within Eurocode, and for completeness. As a constraining parameter on the response spectrum, however, it is evident that in the acceleration domain T_D has far less influence on the shape of the curve. The UHS is not extrapolated to longer periods; hence T_D is limited to the range $T_C \leq T_D \leq 4.0$. Given these limitations it is interesting to see that the spatial pattern of T_D is remarkably consistent with the regional seismotectonics, with the highest values of T_D found in the areas of highest seismic activity and with the potential for larger magnitude ($M_W > 7$) earthquakes. In practice, however, these limitations (particularly the 4 s upper limit) are severe, and result in T_D values that are lower than those found in previous estimates. For low seismicity regions T_D generally seems to fall within the range 1.0 to 1.4 s, which would suggest that the recommended value of 1.2 s for the Eurocode 8 Type II spectrum may be appropriate here.

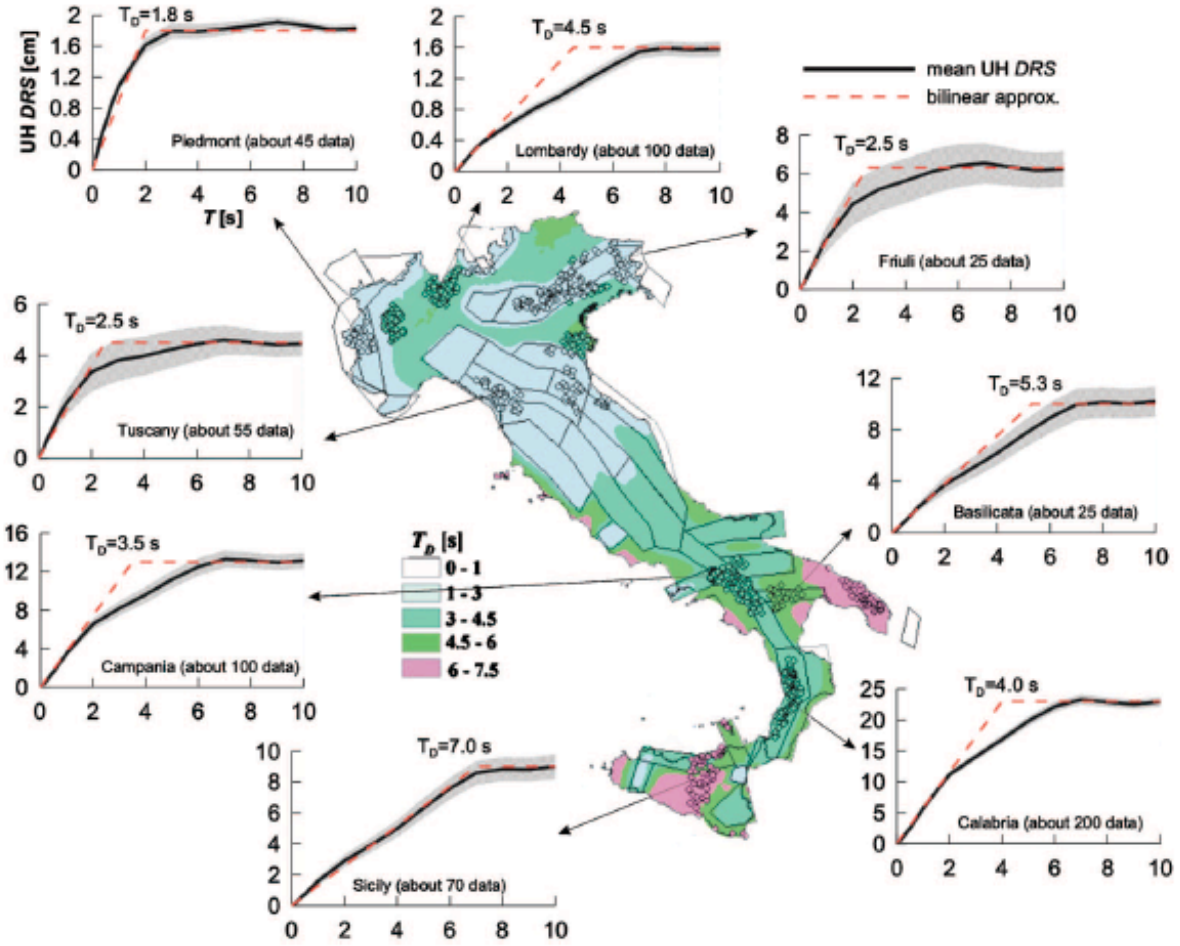

Figure 3.9 Map of spatial variation of T_D within Italy, derived using a uniform hazard displacement spectrum (Faccioli & Villani, 2009)

As a means of comparison, the map of T_D values for Italy produced by Faccioli & Villani (2009) is shown in Figure 3.9. The T_D values shown in Figure 3.9 are derived from a bilinear approximation to the displacement spectrum, calculated from a hazard analysis using the Cauzzi & Faccioli (2008) and Boore & Atkinson (2008) ground motion prediction equation. It should be noted that for parts of northern Italy the values of T_D in the range of about 1.8 to 2.5 s are not inconsistent with the estimates using the optimisation approach. Likewise for parts of southern Italy we find T_D values in the 3 – 4 s range. Where this is a clear distinction is in the very large T_D values in the Apulia region of Italy and in southern and western Sicily. Whilst Figure 3.9 is in agreement that the largest values of T_D are found in Apulia, the values suggested by Faccioli & Villani (2009) are greater than the range it is possible to fit at present. For Sicily, however, we observe a different pattern altogether, the reasons for which are not clear and may possibly be attributed to differences in the characterisation of the earthquake source or the selection of ground motion prediction equation. It is reasonable to speculate that if the methodology of Faccioli & Villani (2009) were applied in the Aegean region, even higher values of T_D may be expected.

To improve the constraint of the T_D parameter, there are several options that could be explored. The first is to simply extend the period range considered in the probabilistic seismic hazard analysis and to either i) continue with the present optimisation strategy, albeit with a higher upper bound, or ii) extend the optimisation strategy to fit a bilinear model to the

displacement spectrum (subject to the constraint $T_C \leq T_D \leq \max(T)$). Alternatively, it may be appropriate to adopt the approximation suggested by Faccioli & Villani (2009):

$$T_D = \frac{2\pi D_{10}}{\max PSV} \tag{3.4}$$

where D_{10} is the value of the uniform displacement spectrum at 10 s, and max PSV is the maximum pseudo-spectral velocity inferred from the uniform hazard spectrum. In either case it would be necessary to calculate the uniform hazard spectra for periods up to 10 s. As only two of the selected GMPEs for active shallow regions can be used for very long periods the decision was made to limit the returned spectral ordinates to 4 s using the current logic tree. It may therefore be necessary to provide separate estimates of T_D using a smaller logic tree or single branch taking only the Cauzzi & Faccioli (2008) or Chiou & Youngs, (2008) GMPE in active shallow regions.

To test the comparison between the present methodology and that proposed by Faccioli & Villani (2009), the UHS has been extended in active shallow seismicity regions to include periods up to 10 s. To achieve this, the seismic hazard for long period spectral acceleration was undertaken using a logic tree with only two GMPE: Cauzzi & Faccioli (2008) and Chiou & Youngs (2008), with both given a weighting of 0.5. Only the active shallow branch of the logic tree is considered. Maps of 10 s spectral displacement, and the corresponding T_D estimate, for Europe defined using equation 3.4, are shown in Figures 3.10 and 3.11.

In Figure 3.11 we observe a similar trend in T_D for mainland Italy as that shown in Faccioli & Villani (2009), with T_D values in the range of 7 to 8 seconds being observed in the Basilicata region of southeast Italy. For Sicily we do not observe such high values of T_D, as we find the SHARE results suggesting lower accelerations in the central and western Sicily than those presented in previous studies. Given the high seismicity in the Aegean region, it is clearly expected that similarly high values of T_D would be evident on mainland Greece and Turkey. These are in the region of approximately 8 to 9 seconds. The lower T_D values around the north and east Anatolian fault systems are easily accounted for by the controlling earthquake, which when it is in the near-field to the site will see a greater contribution to the hazard at higher frequencies, thus reducing the constant displacement corner period. One very clear anomaly, however, is in the Hellenic Arc and southern Turkey. It is in this area that the largest earthquakes and highest overall seismicity is observed; yet Figure 3.11 shows a very low T_D (comparable to low-moderate seismicity regions). This pattern is an artefact that arises from consideration of only the active shallow branch. As no subduction GMPEs are available that contain coefficients for longer spectral periods, it was not possible to run a comparison for subduction sources. As such sources are dominant in the Hellenic and Cypriot arcs, most of the seismicity is not represented in the calculation of S_d (10 s) in the present example. In reality, one would expect similarly high (or even higher) values of T_D in the Hellenic and Cypriot arcs.

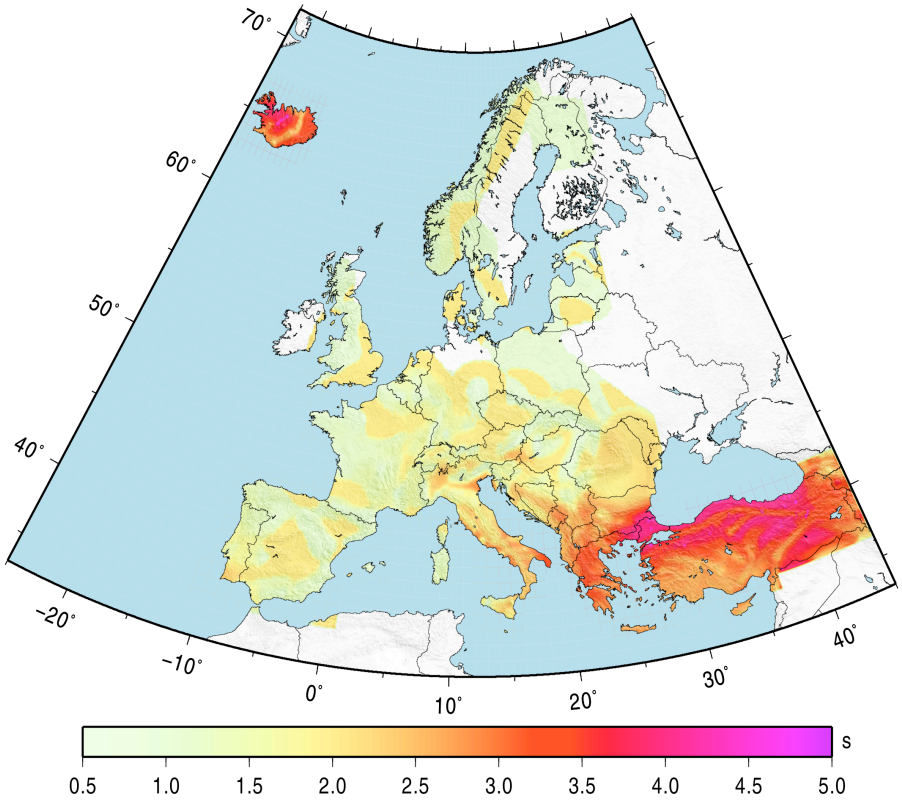

Figure 3.10: 10 second spectral displacement with a 10 % probability of being exceeded in 50 years

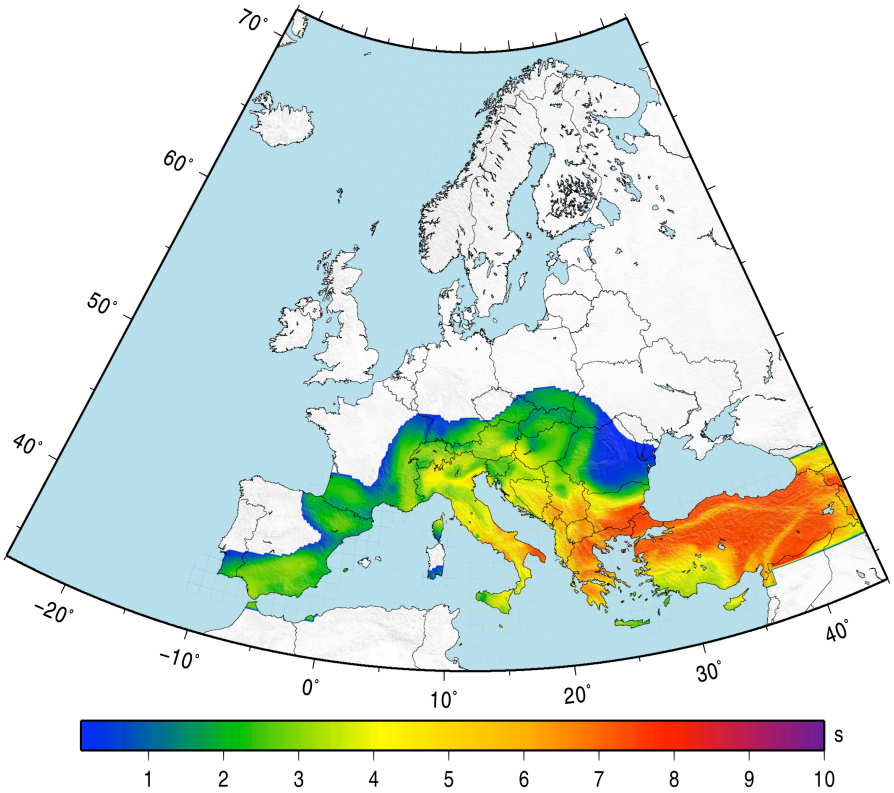

Figure 3.11: Corner period T_D for Europe derived from the S_d(10 s) with a 10 % probability of being exceeded in 50 years, using the method of Faccioli & Villani (2009) (equation 3.4)

3.4. k-value

EN 1998-1 2.1(4) describes the application of the importance factor in order to scale the reference seismic action to different probability levels. Within this provision is included the following note:

At most sites the annual rate of exceedance, $H(a_{gR})$, of the reference peak ground acceleration a_{gR} may be taken to vary with a_{gR} as: $H(a_{gR}) \sim k_0 a_{gR}^{-k}$, with the value of the exponent k depending on seismicity, but being generally of the order of 3. Then, if the seismic action is defined in terms of the reference peak ground acceleration a_{gR}, the value of the importance factor γ_I multiplying the reference seismic action to achieve the same probability of exceedance in T_L years as in the T_{LR} years for which the reference seismic action is defined, may be computed as $\gamma_I \sim (T_{LR}/T_L)^{-1/k}$. Alternatively, the value of the importance factor γ_I that needs to multiply the reference seismic action to achieve a value of the probability of exceeding the seismic action, P_L, in T_L years other than the reference probability of exceedance P_{LR}, over the same T_L years, may be estimated as $\gamma_I \sim (P_L/P_{LR})^{-1/k}$.

This note suggests of a scaling factor (k ~ 3) to be applied to increase or decrease the reference hazard level. The appropriateness of the scaling factor is discussed in SHARE Deliverable 2.2, although the opportunity may be taken to consider this with the new results. The SHARE hazard results do, however, provide an opportunity to determine the extent to which the approximation k ~ 3 is appropriate to a given site. Therefore a map of k-value is shown in Figure 3.13a for PGA.

Figure 3.12 shows hazard curves for selected sites of high and low hazard in different regions of Europe, deliberately selected as sites where estimates of *k*-value have been made in previous studies (H. Bungum, *personal communication*). Arguably the most important observation to note is that the linear approximation of the hazard curve in log-log space is limited to a very narrow range of probabilities, if indeed it can be made at all. Consequently, the derivation of the *k*-value is highly dependent on the probability range being considered. In the absence of explicit guidance on the derivation of this parameter, we fit the linear model only to the range of probabilities considered in the typical design code application. Therefore the line is fit to a limited number of hazard data points corresponding to return periods between 70 years and 5000 years. In some cases this will result in too few data points for a simple linear regression, where such sites are indicated as null or no/data in the subsequent *k*-value maps. In each of the curves the approximate linear model and the corresponding *k*-value are indicated. Over the relatively narrow range of probabilities considered here, it can be seen that the linear model is not necessarily a poor approximation to the hazard curve, with some possible exceptions in very low seismicity regions.

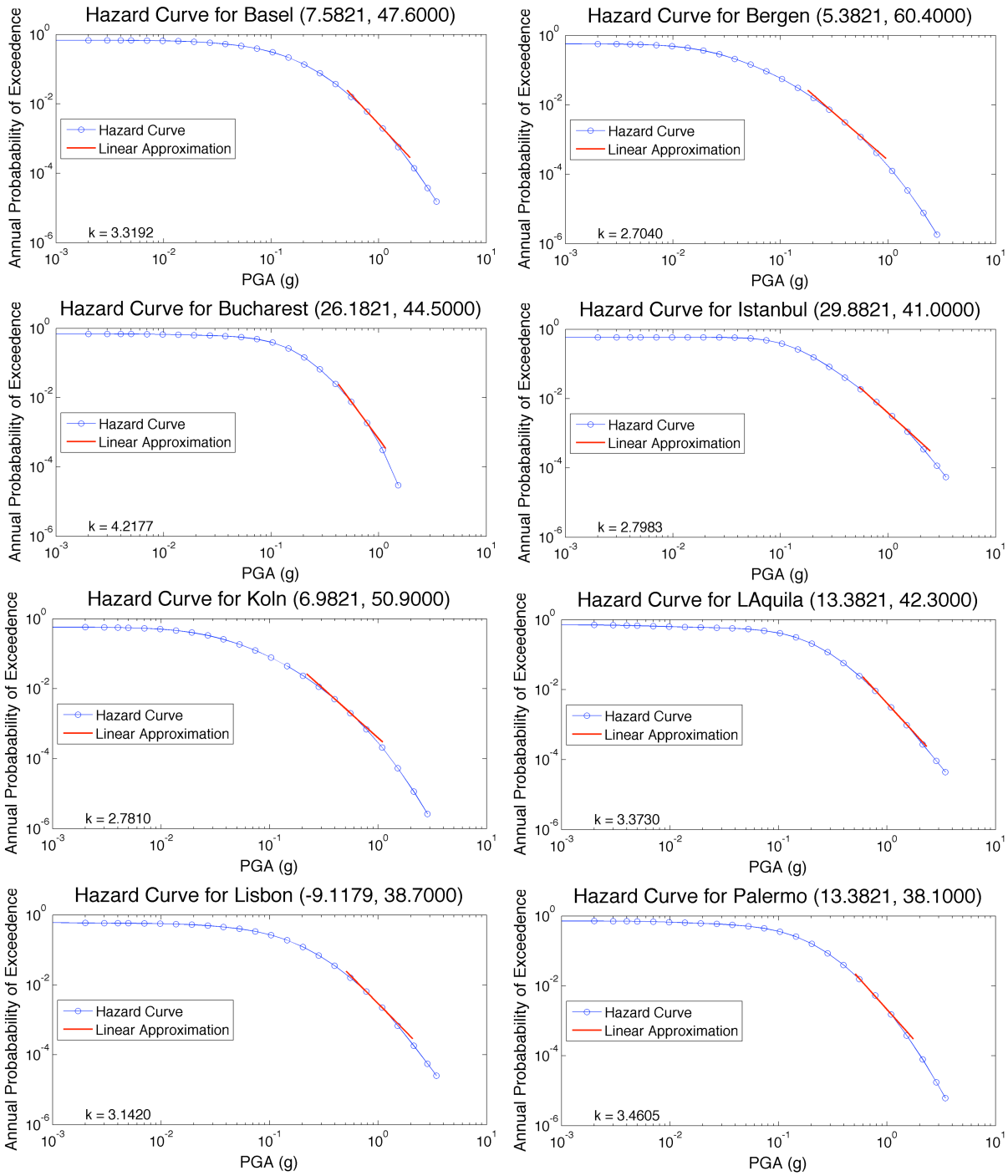

Figure 3.12 PGA hazard curves for selected sites across Europe, with linear model approximation shown as a red line (continued overleaf ...)

From the comparison of hazard curves and the corresponding k-value fits (with the linear approximation anchored to the 475 year return period value) it can be seen that whilst the linear approximation is not itself a poor approximation over the limited return period range, the value of *k* is closely linked with the shape of the hazard curve. In higher hazard areas the hazard curves are showing a more linear behaviour in the 70 to 5000 year return periods, whereas in lower regions there is greater curvature within this return periods range. This effect largely explains the spatial trend observed in Figure 3.13a, in which *k*-values are in the

range of 2.0 to 3.0 in low seismicity regions, compared to 3.0 to 4.0 in higher seismicity regions.

In addition to being a spatially variable parameter, *k*-value also varies over the spectral period. Maps of *k*-value for the 0.2 s and 1.0 s spectral acceleration hazard curves are shown in Figure 3.13b and 3.13c. Whilst the spatial trend of *k*-value does not appear to change at longer periods, there is a general tendency toward lower *k*-value at higher spectral periods.

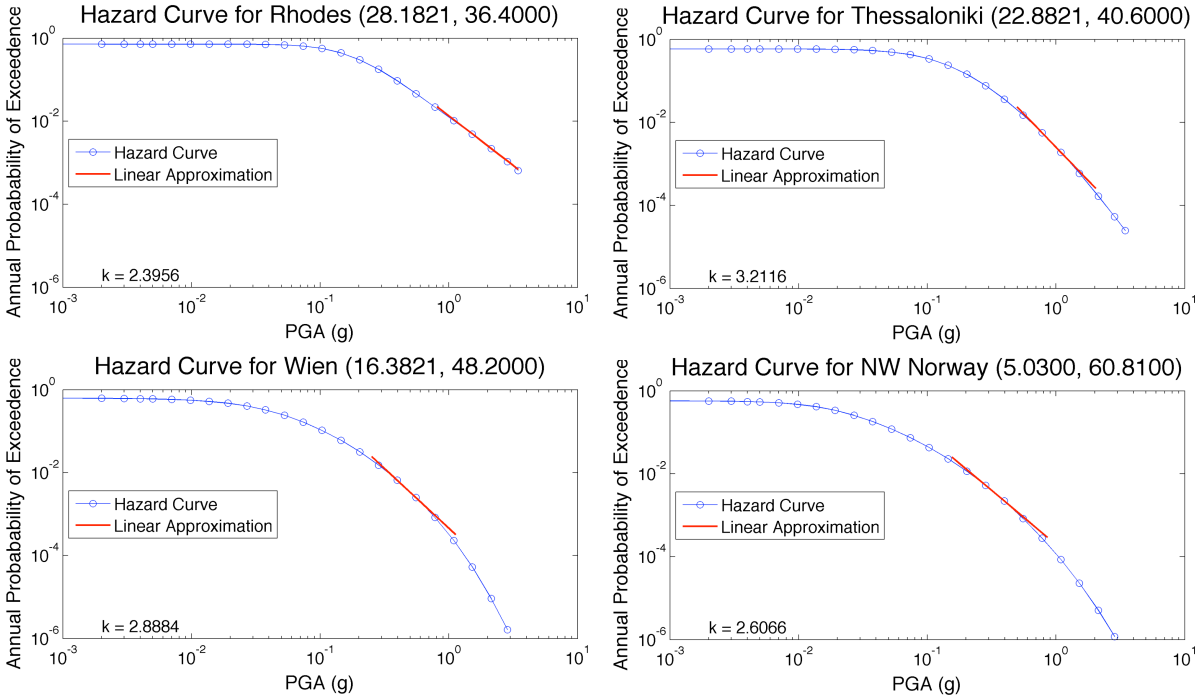

Figure 3.12 ... continued.

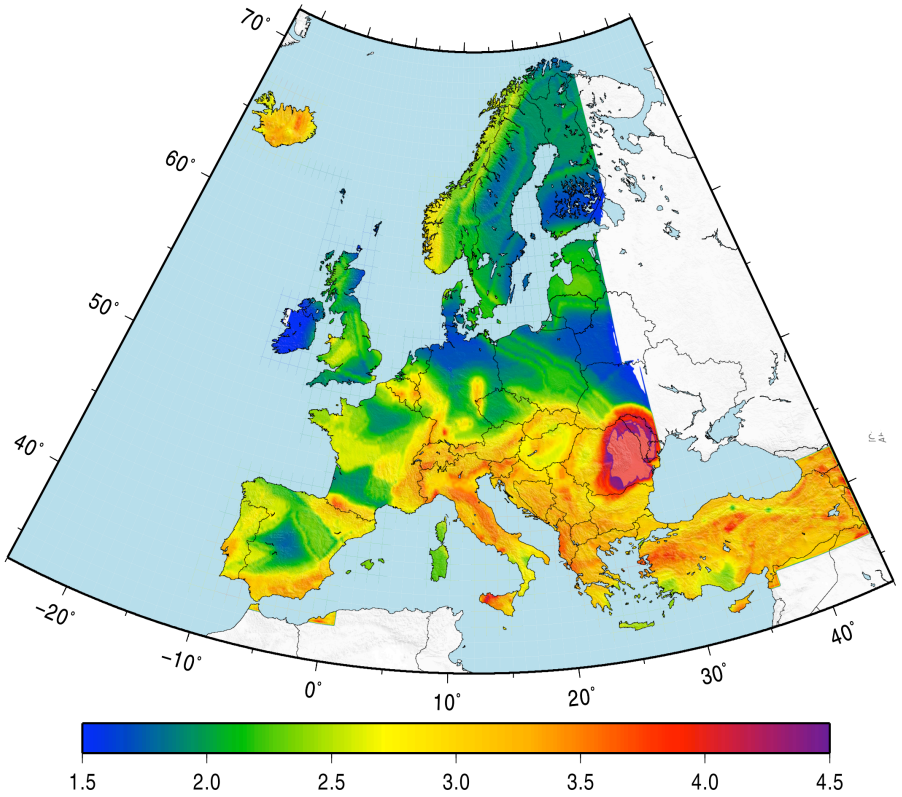

Figure 3.13a: Variation in k-value for PGA hazard

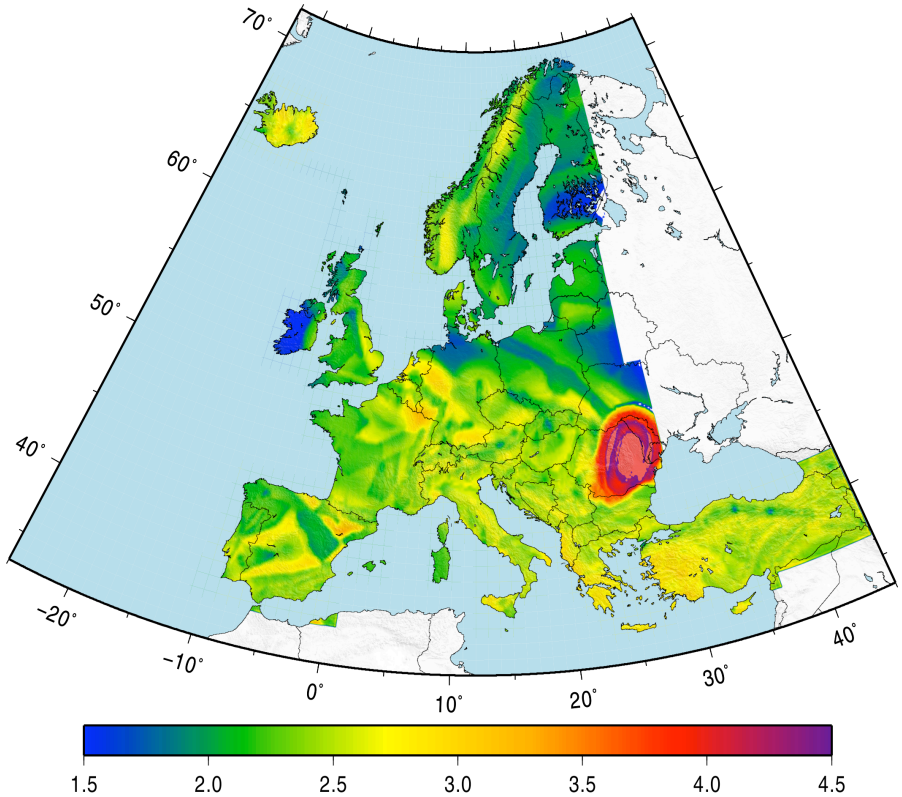

Figure 3.13b: Variation in k-value for Sa (1.0 s) hazard

4. SCALAR QUANTIFICATION OF HAZARD SPECTRA

The definitions of the Eurocode 8 design spectrum parameters from the UHS, by means outlined in this section, have so far considered each of the parameters separately. This is to illustrate how such parameters may vary across Europe, which is of great relevance when considering potential modifications to the recommended values of F_0, T_B, T_C and T_D by National Annexes. For delineating the zones, however, the treatment of the controlling parameters separately makes a general estimation of the variation in hazard more complex. An alternative is to consider the use of a metric that is influenced by both the strength of the ground motion and the shape of the spectrum, or to be more precise the strength of ground motion intensity across the spectrum. For this, we make use of two parameters: pseudo-velocity spectrum intensity (VSI) (Housner, 1959) and Acceleration Spectrum Intensity (ASI). These parameters are derived from any ground motion response spectrum according to:

$$VSI(\xi) = \int_{T=0.1}^{T=2.5} PSv(T,\xi) \tag{3.5a}$$

and

$$ASI(\xi) = \int_{T=0.1}^{T=0.5} Sa(T,\xi) \tag{3.5b}$$

Where $PSv(T, \xi)$ and $Sa(T, \xi)$ are the pseudo-spectral velocity and spectral acceleration, respectively, of a single degree-of-freedom (SDOF) oscillator with natural period T and coefficient of damping ξ.

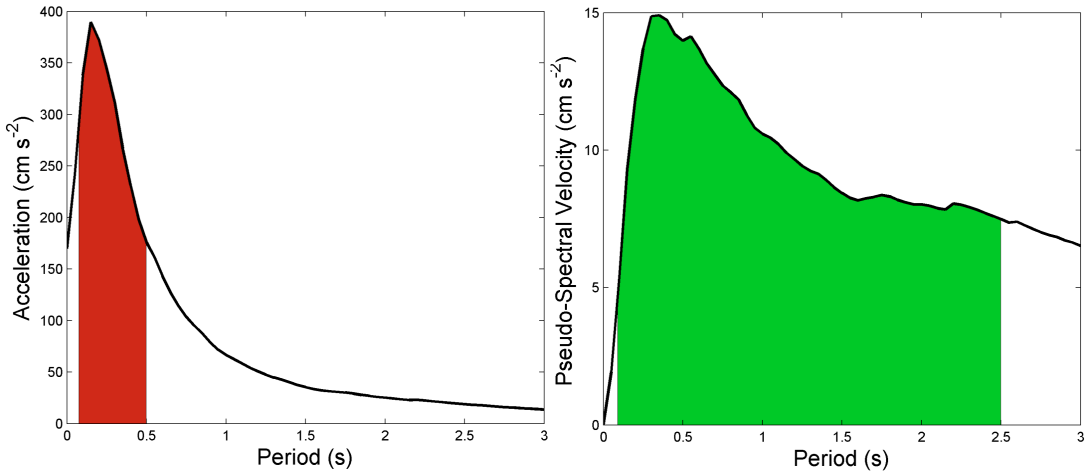

Figure 3.14: Area of the integral of the response spectrum for ASI (left) and Pseudo-VSI (right)

To illustrate the principals of VSI and ASI, Figure 3.14 demonstrates their more common application to strong ground motion response spectra. As a scalar metric of ground motion, both the ASI and VSI will increase in proportion to the total energy of the ground motion. Whilst these metrics are traditionally defined for a single record of ground motion, the theoretical principals underpinning their usage do not necessarily preclude them from being applied to uniform hazard spectra. This is, of course, with the obvious caveat that the UHS in itself is not representative of the spectrum emerging from a single earthquake.

Figures 3.15 and 3.16 illustrate how VSI and ASI, when applied to the pseudo-spectral velocity and acceleration uniform hazard spectra, vary across Europe. Their pattern spatial pattern is consistent with the concept that VSI and ASI are representative of the scale of "overall" hazard, elucidating the contrast between low and high hazard areas of Europe. For the purpose of outlining the spatial trend, there is little difference between VSI and ASI.

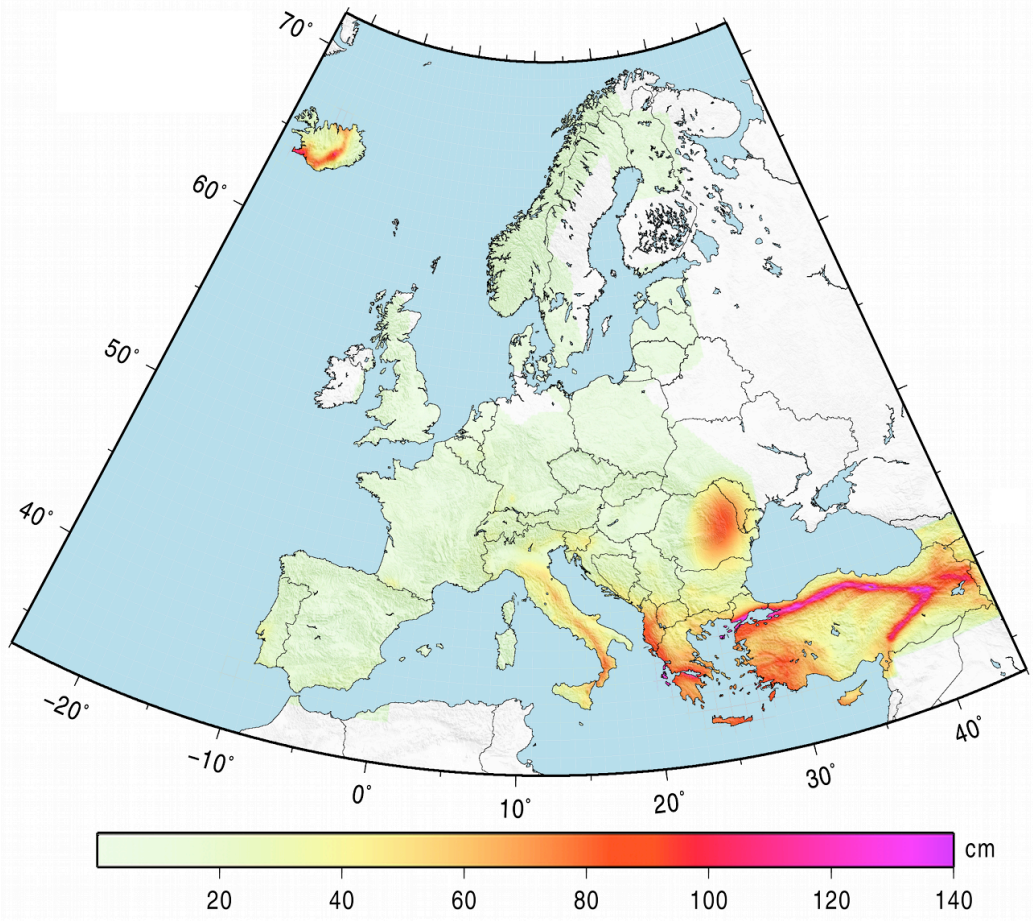

Figure 3.15: Variation in Pseudo-VSI, with a 10 % probability of being exceeded in 50 years, across Europe from the SHARE model

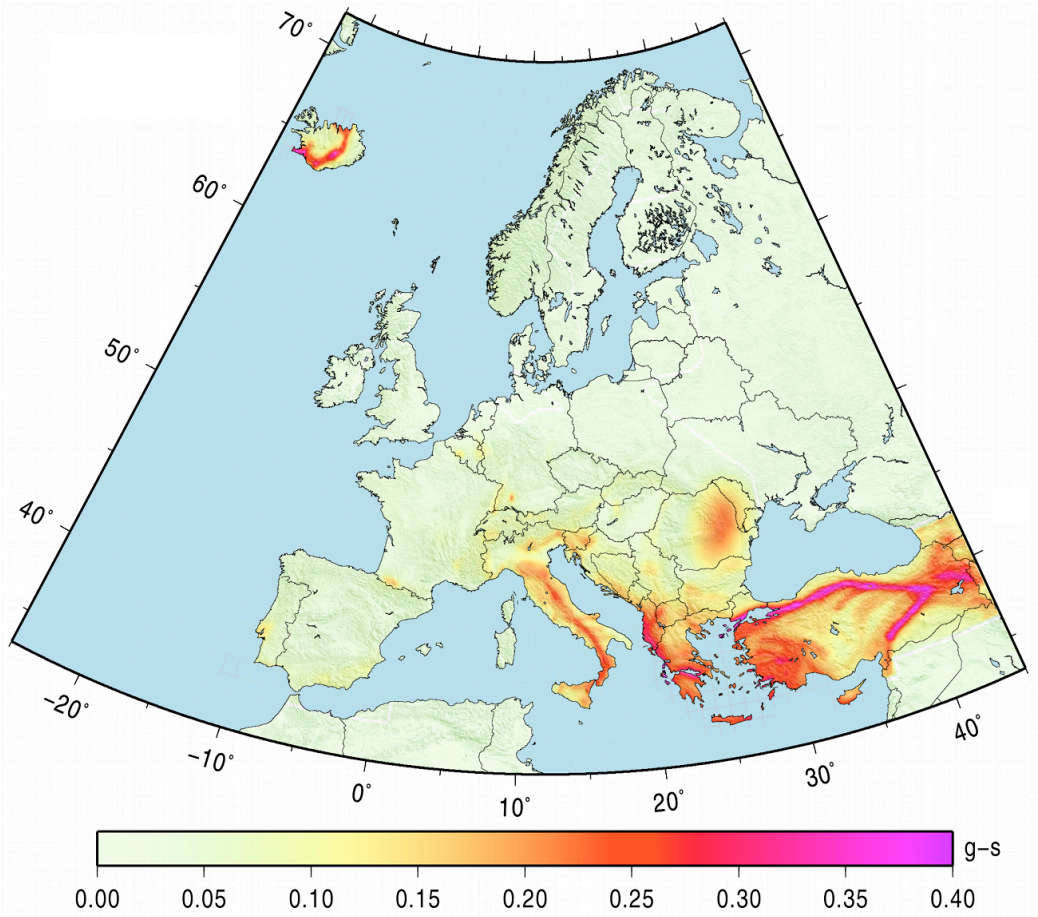

Figure 3.16: Variation in ASI, with a 10 % probability of being exceeded in 50 years, across Europe from the SHARE model

5. Preliminary Zonation

For the characterisation of the seismic hazard in Europe, the preliminary zonation is defined as a composite of the peak ground acceleration with a 10 % probability of being exceeded in 50 years (Figure 4.1a), and the 4.0 s spectral displacement with a 10 % probability of being exceeded in 50 years (Figure 4.1b).

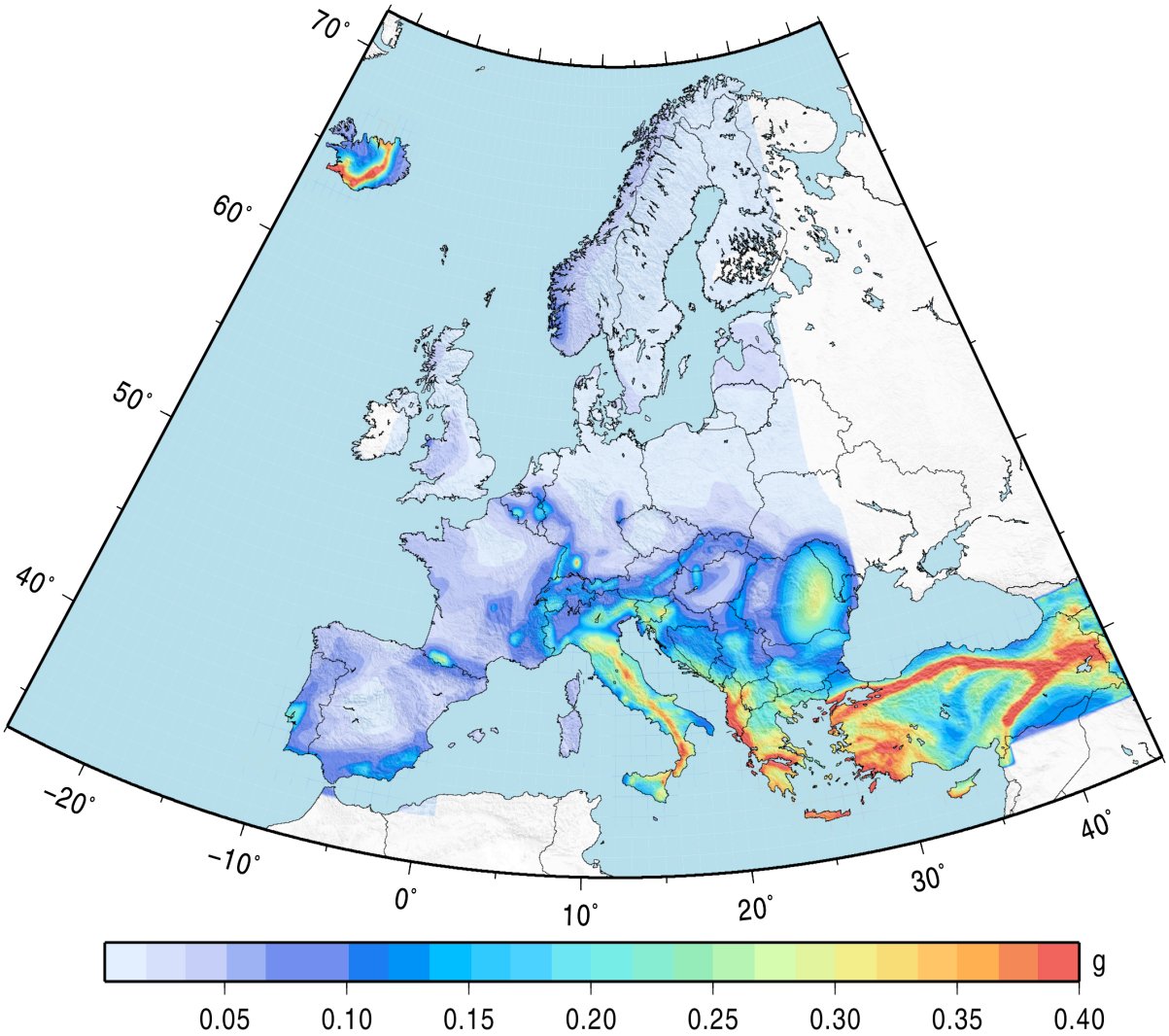

Figure 4.1a. Zonation component 1: PGA with a 10 % probability of being exceeded in 50 years

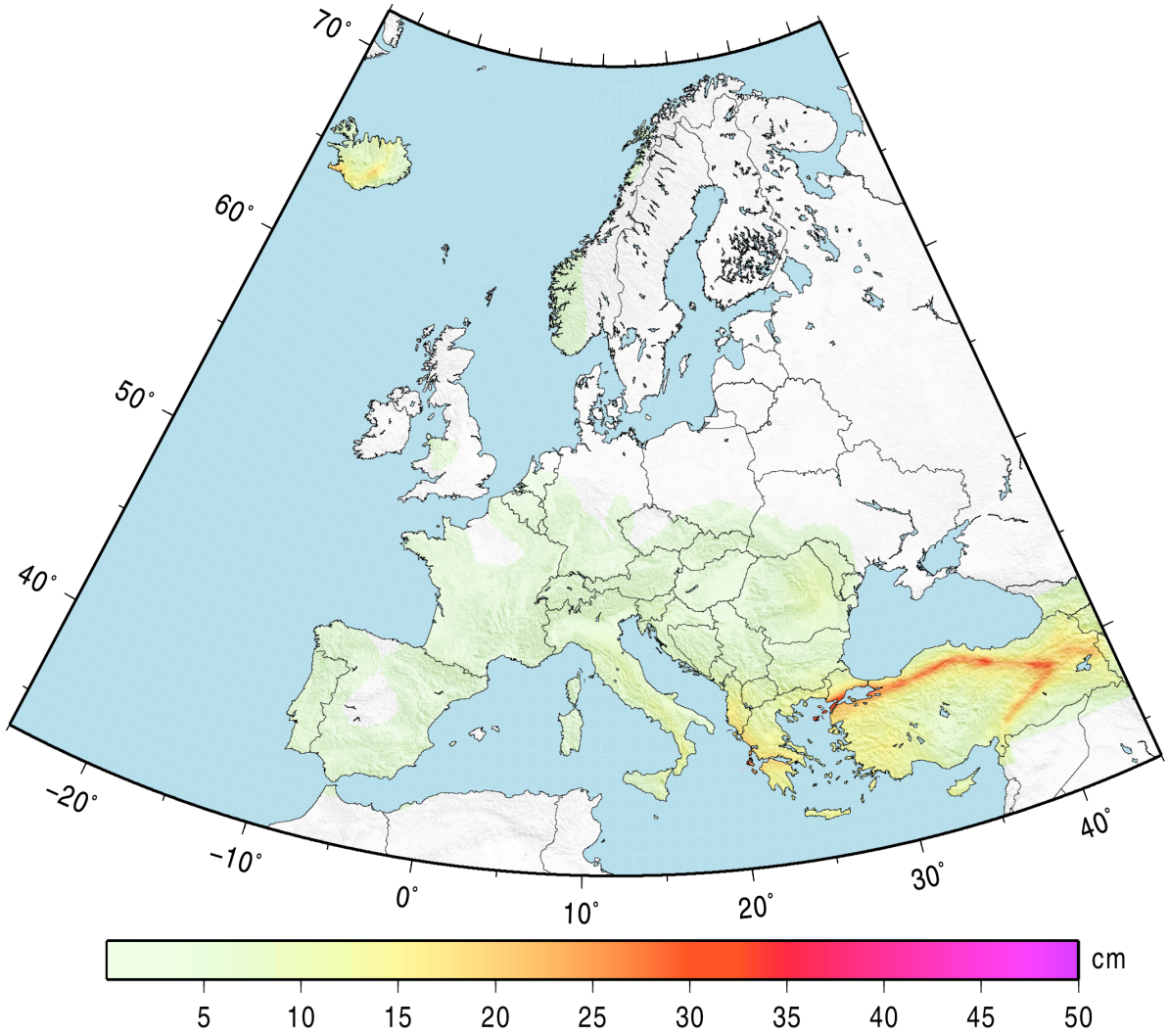

Figure 4.1b. Zonation component 2: S_d (4.0 s) with a 10 % probability of being exceeded in 50 years

The maps shown in Figure 4.1 provide a broadly qualitative overview of the spatial variation in hazard. The PGA hazard map largely defines the hazard in the manner that is consistent with the current Eurocode 8 definition. By contrast the 4.0 s spectral displacement is more representative of the spatial variation in hazard as it might pertain to engineered structures. The latter is more heavily controlled by the occurrence of larger events; hence, the most active regions of western Greece and northwest Turkey stand out more clearly. The definition of seismic zones across Europe can, and should, be refined further within each region to take into the spatial variations in the design spectrum parameters (shown in section 3).

As a longer term objective, the output from the SHARE project and its dissemination provide an opportunity to consider the adoption of provisions explicitly requiring the use of hazard curves and uniform hazard spectra to characterise the seismic input needed for design in Europe. Precedents for such an approach are already found in recent building design codes from the United States and Canada.

Acknowledgements

The authors would like to acknowledge the support provided by the European Commission under FP7 through the financing of the SHARE (Seismic Hazard Harmonisation in Europe) research programme, under the framework of which this work has been funded. Feedback and contributions on some of the work relating to this topic was provided from Hilmar Bungum, Domenico Giardini, Ezio Faccioli, Kyriazis Pitilakis, Artur Pinto, Roberto Paolucci, Martin Koller and Manualla Villani.

References

Bommer, J. J., and Alarçon, J. (2006) The Prediction and Use of Peak Ground Velocity. *Journal of Earthquake Engineering*. 10(1). 1 – 31

Bommer, J. J., Stafford, P., and Akkar, S. (2010) Current Empirical Ground Motion Prediction Relations and their Application in Eurocode 8. *Bulletin of Earthquake Engineering*. 8. 5 - 26

Boore, D. M., and Atkinson, G. A. (2008). Ground-Motion Prediction Equations for the Average Horizontal Component of PGA, PGV, and 5%-Damped PSA at Spectral Periods between 0.01 s and 10.0 s. *Earthquake Spectra*, 24(1). 99 - 138

Cauzzi, C. and Faccioli, E. (2008). Broadband (0.05 to 20.0 s) prediction of displacement response spectra based on worldwide digital records. *Journal of Seismology.* 12, 453 - 475

Chiou, B., S-J., Youngs, R. R., (2008) An NGA Model for the Average Horizontal Component of Peak Ground Motion and Response Spectra. *Earthquake Spectra*. 24(1)**.** 173 – 215

Crowley, H., Weatherill, G. and Pinho, R. (2013). Suggestions for Updates to the European Seismic Design Regulations. SHARE Deliverable 2.6. 1 - 11

Faccioli, E., and Villani, M. (2009). Seismic Hazard Mapping for Italy in Terms of Broadband Displacement Response Spectra. *Earthquake Spectra*. 25(3)**.** 515 – 539.

Garcia-Mayordomo, J., Faccioli, E. and Paolucci, R. (2004) Comparative Study of the Seismic Hazard Assessment in European National Seismic Codes. *Bulletin of Earthquake Engineering*. 2**.** 51 - 73

Solomos, G., Pinto, A. and Dimova, S (2008) A Review of the Seismic Hazard Zonation in National Building Codes in the Context of Eurocode 8: Support to the implementation, harmonization and further development of the Eurocodes. JRC Scientific and Technical Reports.

Weatherill, G., Crowley, H. and Pinho, R. (2010) Report on seismic hazard definitions needed for structural design applications. SHARE Deliverable 2.2. 1 - 164